*American Journal of Nanomaterials, 2018, Vol. 6, No. 1, 15-23*
Available online at http://pubs.sciepub.com/ajn/6/1/2

DOI:10.12691/ajn-6-1-2

# Recent Advances of ZnO Based Nanowires and Nanorods Devices

**Ahmed M. Nahhas***

Department of Electrical Engineering, Faculty of Engineering and Islamic Architecture,
Umm Al Qura University, Makkah, Saudi Arabia
*Corresponding author: amnahhas@uqu.edu.sa

**Abstract** This paper presents the recent advances of the Zinc Oxide (ZnO) based nanowires and nanorods devices. ZnO has gained a substantial interest in the research area of the wide bandgap semiconductors due to its unique electrical, optical and structural properties. ZnO is considered as one of the major candidates for electronic and photonic applications. Also, it has distinguished and interesting electrical and optical properties. ZnO is considered as a potential contender in optoelectronic applications such as solar cells (SCs), surface acoustic wave devices, and ultraviolet (UV) emitters. The ZnO as a nanostructured material exhibits many advantages for nanodevices. ZnO nanostructured material has the ability to absorb UV radiation and immense in many optical applications. Recently, ZnO nanostructured based devices have gained much attention due to their various potential applications. ZnO as nanomaterial has been used in many devices such as UV photodetectors (PDs), light emitting diodes (LEDs), and transistors. The recent aspects of ZnO nanowires and nanorods based devices are presented and discussed.

***Keywords:*** *ZnO, Gallium nitride (GaN), nanostructured, doping, LEDs, nanowires, nanorods, UV*

**Cite This Article:** Ahmed M. Nahhas, "Recent Advances of ZnO Based Nanowires and Nanorods Devices." *American Journal of Nanomaterials*, vol. 6, no. 1 (2018): 15-23. doi: 10.12691/ajn-6-1-2.

## 1. Introduction

ZnO is an *n*-type semiconductor material, falls in group II-VI. It is in between covalent and ionic bond of semiconductor. ZnO has a wide bandgap of 3.37 eV and high binding energy of 60 meV at room temperature [1]. Also, ZnO has some other interesting properties such as high exciton binding energy, thermal stability, environmental compatibility, high mechanical and optical gain, and radiation hardness [2]. These properties made ZnO a leading material for several electronic and optoelectronic devices. The high binding energy permits the fabrication of ZnO based photo-electronic devices possessing high optical efficiency, while the wide bandgap eases the application of ZnO thin films for short wavelength optoelectronic devices [3].

ZnO has a good optical transparency in the visible wavelength region [4]. ZnO is considered as one of the major candidates for electronic and photonic applications due to its excellent optical and electrical characteristics. Due to its distinguishing features and interesting optoelectronic properties, ZnO is considered as a potential contender in optoelectronic applications such as SCs, surface acoustic wave device, and UV emitters [5,6,7]. These characteristic properties attracted several researchers to improve the electrical and optical properties of the ZnO thin films. Other physical properties opened a wide range of applications in photovoltaics, LEDs, PDs in UV spectral range, and microelectromechanical systems (MEMs) [8,9,10,11,12]. The ZnO crystalline structure exists as wurtzite and zinc blende as shown in Figure 1, which led it as a perfect polar symmetry along the hexagonal axis, which is responsible for a number of physical and chemical properties, including piezoelectricity and spontaneous polarization [13].

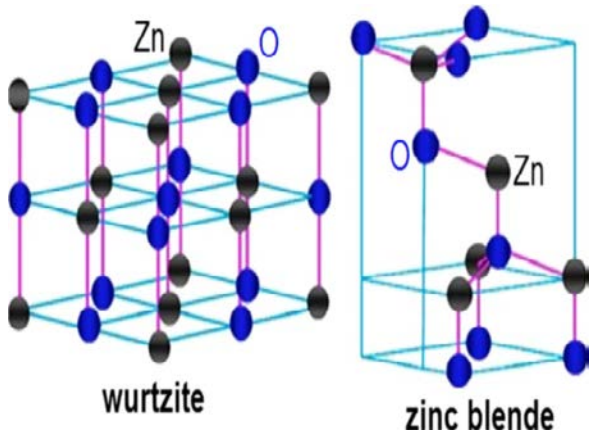


**Figure 1**. ZnO wurtzite structure [3]

## 2. ZnO Doping

Normally, doping is used to improve the structural, optical and electrical properties of pure ZnO thin films [14]. The intrinsic ZnO is *n*-type due to oxygen vacancies and thus, doping it with *p*-type dopants has proven to be extremely difficult. However, *p*-type impurities can

potentially reduce the charge leakage and electron screening effect [15]. Among the *p*-type dopants, lithium (Li) is an excellent candidate because it can take off centered positions by replacing Zn atoms in the wurtzite structure [16].

ZnO epilayers are usually found to be unintentionally *n*-type conducting with high electron concentration. This is believed to be the resulting of certain point defects [17]. This is one of the reasons for a reliable and a reproducible *p*-type ZnO film is difficult to achieve. The *p*-type doping is considered one of the biggest issues to the development of the ZnO based p-n junction devices. GaN is one of the materials that can be used in order to bypass this issue without sacrificing the advantages of ZnO material [18]. GaN is a wide bandgap semiconductor with a very similar lattice constant as ZnO and where *p*-type doping can be reliably achieved with magnesium (Mg) doping, in place of *p*-ZnO [18]. In many applications, the *p*-type doping of the ZnO is desired such as p-n heterojunction structure. There are several reports on ZnO based heterojunctions with *p*-type semiconductors such as silicon (Si) [19], AlGaN [20], or GaN [21]. On the other hand, doping of ZnO with group III elements like aluminum (Al) [22], gallium (Ga) [23], and indium (In) [24] is known to decrease the electrical resistivity significantly caused by an increased free carrier concentration. The used of Al doping due to its nontoxic, inexpensive with high conductance and high transparent in visible range [22].

## 3. ZnO Nanostructured Material

Recently, the deposition of ZnO nanoscale materials with certain morphologies is increasing due to their novel optical and electrical properties and potential applications in the fields of photonic and electronic devices. Substantial efforts have been made for developing the ZnO thin films in different shapes such as nanorods, nanowires, nanocubes and nanobelts [25,26,27,28]. These nanostructured ZnO thin films have potential application in UV laser emission, biosensors, PDs. and LEDs devices. The nanostructured ZnO nanowires and nanorods based devices have attracted a considerable interest due to their importance in potential applications such as electronic, optoelectronics, electrochemical, electromechanical nanodevices [29] and biosensing [30]. Many other applications have been reported for the ZnO based nanostructures, thin films and devices, such as transparent electronics [31], UV light emitters [32], piezoelectric devices [33], p-n junctions [34], field effect devices [35], sensors [36], optoelectronics [37], and field emission devices [38].

## 4. ZnO Nanowires/Nanorods Devices

### 4.1. ZnO Nanowires Devices

ZnO nanowires have attracted extensive research interests for their potential applications in optoelectronic areas. In recent years, many researches have reported on devices based on ZnO nanostructured nanowires because of their high specific surface area, low cost and ease of manufacturing [39,40,41,42]. Several methods are being used for the synthesis of ZnO nanowires such as vapor liquid solid [43], metal organic chemical vapor deposition (MOCVD) [44], chemical bath deposition [45] and hydrothermal method [46]. The quality of the resulted ZnO nanowires fabricated by these methods is varied.

The measurements of the residual carrier concentration on non-intentionally doped ZnO nanowires using the scanning spreading resistance microscopy (SSRM) was reported by Wang et al. [47]. For this purpose, an SSRM calibration profile was developed on homoepitaxial ZnO:Ga multilayer staircase structures grown by molecular beam epitaxy (MBE) [47]. The Ga density was measured by secondary ion mass spectroscopy (SIMS) varies in the 1.7 x $10^{17}$ $cm^{-3}$ to 3 x $10^{20}$ $cm^{-3}$ range. From the measurements on Ga doped multi-layers, a monotonic decrease in SSRM resistance with increasing Ga density was established, indicating SSRM being a well adapted technique for two dimensional dopant/carrier profiling on ZnO at nanoscale [47]. The study's results showed that the residual carrier concentrations of ZnO nanowires were found to be between $10^{18}$ and 3 x $10^{18}$ $cm^{-3}$. The study's results also showed that SSRM can be well adapted for the dopant/carrier profiling in ZnO nanostructure [47]. Figure 2 shows the scan electron microscopy (SEM) image of the as-grown ZnO nanowires [47].

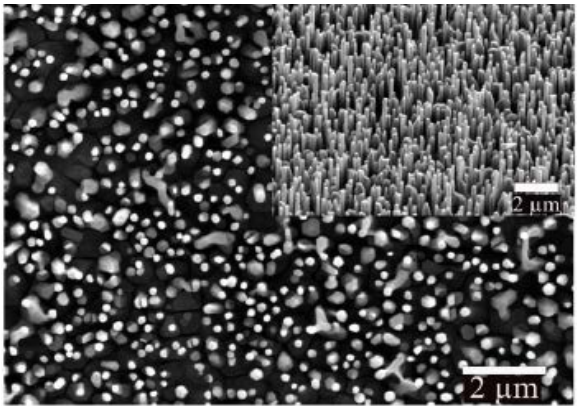


**Figure 2**. SEM image of as-grown ZnO nanowires [47]

The synthesize of the ZnO nanowires using chemical vapor deposition system at 1000°C temperature were reported by Yadav et al. [48]. The as-synthesized ZnO nanowires showed a super hydrophilic nature with water contact angle value of 0°. After dark storage for about 50 days, the nanowires showed a super hydrophobic nature with the contact angle value of about 155° [48]. When these nanowires were exposed to UV light in air atmosphere, the nanowires become a super hydrophilic [48]. It was found that the rate of change of the contact angle depends on the gases atmosphere during the UV light illumination. The rate of change of the contact angle with the UV light illumination was higher in presence of oxygen gas whereas it was very slow in the presence of the hydrogen gas [48]. The study's results showed that the as-synthesized ZnO nanowires were a super hydrophilic in nature [48]. The contact angle increased with the dark storage on the grown ZnO nanowires [48]. The study's results concluded that the presence of the oxygen gas atmosphere or formation of superoxide ions attached on the surface of ZnO

nanowires increased the water wetting in the UV light presence [48]. Figure 3 shows the SEM (a) and the X-ray diffraction (XRD) (b) of the ZnO nanowires [48].

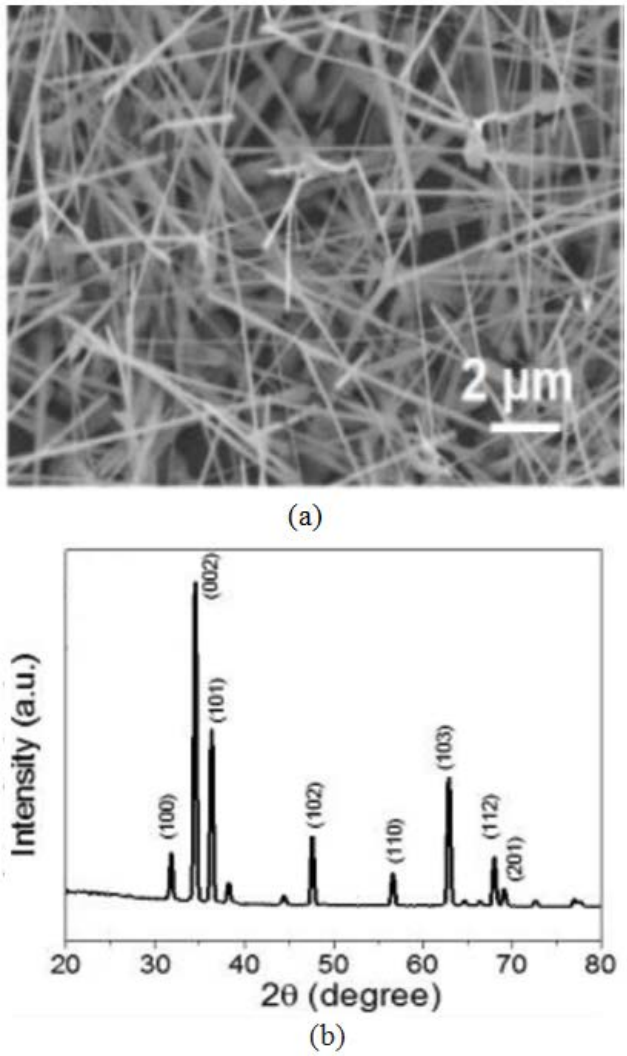


**Figure 3**. (a) SEM image of as-grown nanowires (b) XRD [47]

The ratio influence of Oxygen/Zinc effect on the optical properties in the undoped and doped ZnO nanowires was investigated and reported by Jabri et al. [49]. The photoluminescence (PL) emission line at 3.31 eV in ZnO nanowires was studied [49]. In the undoped ZnO, this band strongly depends on the high oxygen concentration and could originate from the recombination of bound-exciton complex related to the structural defects [49]. Conversely, in doped ZnO, the PL emission appears notably at a low VI/II ratio and with the emergence of donor-acceptor pair emission due to the presence of $\alpha$-No nitrogen complex, which acts as a shallow acceptor in ZnO [49]. It was found that this band corresponds to 3LO, the third phonon replica of resonant Raman scattering (RRS) [49]. Furthermore, a remarkable variation was detected in a number of RRS multi-phonons [49]. Under an excitation wavelength of 351.5 nm, the enhancement of multiple-phonon RS up to n = 4 was observed in the doped ZnO nanowires [49]. This phenomenon was attributed to the incorporation of the nitrogen impurity [49]. The defects presence and/or intermediate electronic states could stimulate the presence of PL band at 3.31 eV and high order RRS processes [49]. It was also found that $\alpha$-No nitrogen complex as a shallow acceptor could not overcome the compensation effect of No under O-rich condition making the formation of this complex less probable [49]. Figure 4 shows the SEM for the ZnO nanowires [49].

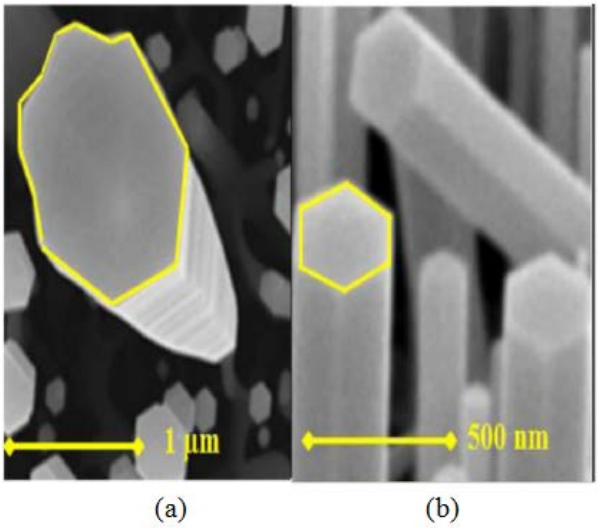


**Figure 4.** SEM images of ZnO nanowires: (a) undoped (b) doped [48]

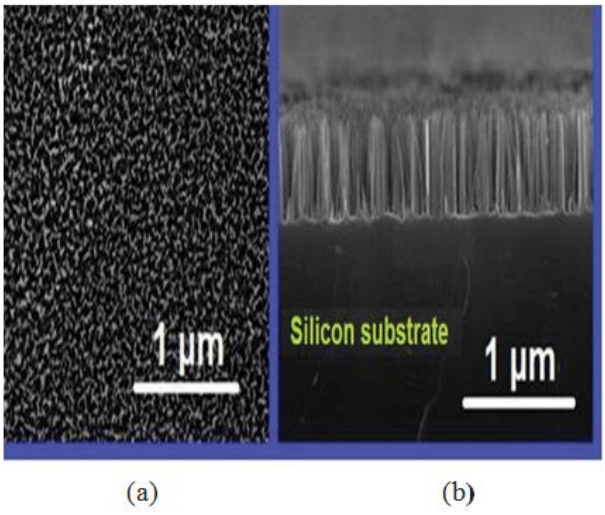


**Figure 5**. Top-view (a) and cross-sectional (b) FESEM image of bare Si nanowires [50]

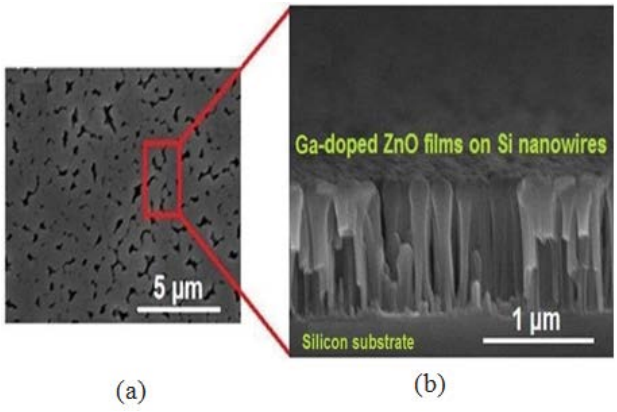


**Figure 6**. (a) Top-view (b) cross-sectional FESEM image of Ga-doped ZnO thin film coated onto Si nanowire arrays [50]

The temperature dependent electrical properties of *n*-type Ga-doped ZnO thin film *p*-type Si nanowire heterojunction diodes were investigated and reported by Akgul et al. [50]. The metal assisted chemical etching (MACE) process was performed to fabricate Si nanowires [50]. In that study, the Ga-doped ZnO films were deposited onto the nanowires through chemical bath deposition (CBD) technique to build three dimensional nanowire based heterojunction diodes [50]. The fabricated devices revealed significant diode characteristics in the temperature range of 220-360 K [50]. The electrical measurements showed that diodes had a well-defined rectifying behavior with a good rectification ratio of $10^3$ ±3 V at room temperature [50]. Ideality factor (*n*) were changed from 2.2 to 1.2 with the increasing of the temperature [50]. The fabricated nanodevices showed good p-n characteristics in the dark conditions at room temperature [50]. The observed diode performance in that study clearly showed that the fabricated device structure could be a promising alternative candidate for high performance low cost optoelectronic device applications in future [50]. Figure 5 shows the top view (a) and cross-sectional (b) field emission scanning electron microscopy (FESEM) image of bare Si nanowires. The top view and the cross-sectional FESEM image for the Ga-doped ZnO thin film coated onto Si nanowire arrays are shown in Figure 6 (a) and (b) [50].

## 4.2. ZnO Nanorods Devices

ZnO nanorods have attracted much interest in various optoelectronic nanoscale devices such as photovoltaic cells [51], UV laser diodes (LDs) [52], LEDs, optical sensors, and UV PDs [53]. For many applications, it is preferable to have large surface area of ZnO. One of the simplest methods for increasing the surface area is growing ZnO nanorods on the ZnO layers. By growing the nanorods, it is expected that the surface area becomes larger, thus more photon energy can be absorbed [54]. The post-annealing process may affect the crystalline structure as well as the PL spectra of ZnO nanorods [54]. ZnO nanorods can be fabricated by different methods including hydrothermal method [55], MOCVD method [56], pulsed laser deposition (PLD) method [57], aqueous solution method [58]. In these methods, the morphology, the microstructure, the optical and the electrical properties of ZnO nanorods are determined by process parameters such as deposition time, deposition temperature, and annealing condition.

The precursor concentration effect on morphology, elemental composition, and structure of ZnO nanorods grown on chromium/gold (Cr/Au) glass substrate were investigated and reported by Mustafa et al. [59]. ZnO nanorods with clear hexagonal shapes from a lower precursor concentration (1mM-9 mM) were produced [59]. ZnO nanorods with different shapes and sizes were prepared on the Cr/Au glass substrate through the hydrothermal method [59]. The concentration's effect of the equimolar solution on the synthesis of ZnO nanorods was investigated [59]. The ZnO nanorods growth were characterized by using FESEM, energy dispersive X-ray spectroscopy (EDX), and XRD to investigate the surface morphology, the elemental and the structure analysis, respectively [59]. It was observed that the precursor concentration has a significant influence on the morphology and the crystal structure, the crystal size, and the FWHM of ZnO nanorods [59]. ZnO nanorods were grown in a high density with an orientation along c-axis of the substrate [59]. It also exhibited the hexagonal structure with a dominant (002) peak in XRD spectrum and possesses a high crystal quality [59]. The concentration effect on atomic percentage of constituent atoms was also studied. The atomic percentage ratio of Zn to O change from 32.5: 67.5 to 48:52 as the precursor concentration increase 1-9 mM. The FESEM and the XRD results clearly showed that a good quality of ZnO nanorods was grown [59]. At certain concentrations, hexagonal nanorods were observed. The seed layer introduction of Cr-Au on the substrate not only controls the density but also promoted the overall orientation of nanorods [59]. The crystal size and the atomic ratio of the constituent elements were also affected by the overall precursor concentration [59]. From 1-5 mM the increase in (002) peak intensity confirmed the improvement of the orientation and the aspect ratio of the ZnO nanorods [59]. The decrease in (002) peaks after 5 mM concentration was due to the small amount presence of the impurities and the poor orientation [59]. The EDX spectrum confirmed the presence of the zinc and oxygen only [59]. Figure 7 (a) shows the SEM for the ZnO nanorods [59]. Figure 7 (b) shows the XRD patterns of ZnO nanorods formed Cr-Au coated glass at different concentrations [59].

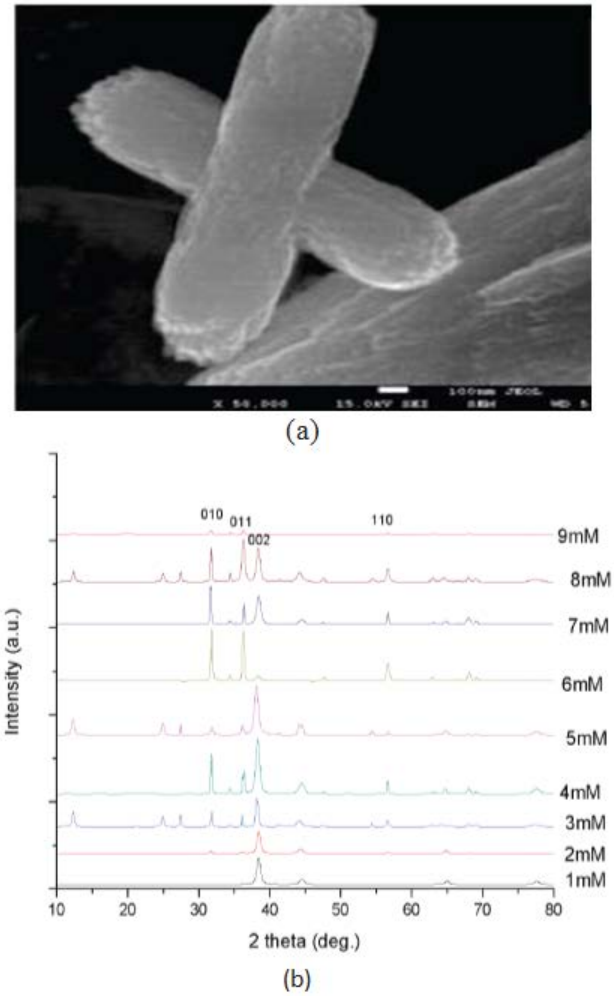


**Figure 7**. (a) SEM for ZnO nanorods [59], (b) XRD patterns of ZnO nanorods formed Cr-Au coated glass at different concentrations [59]

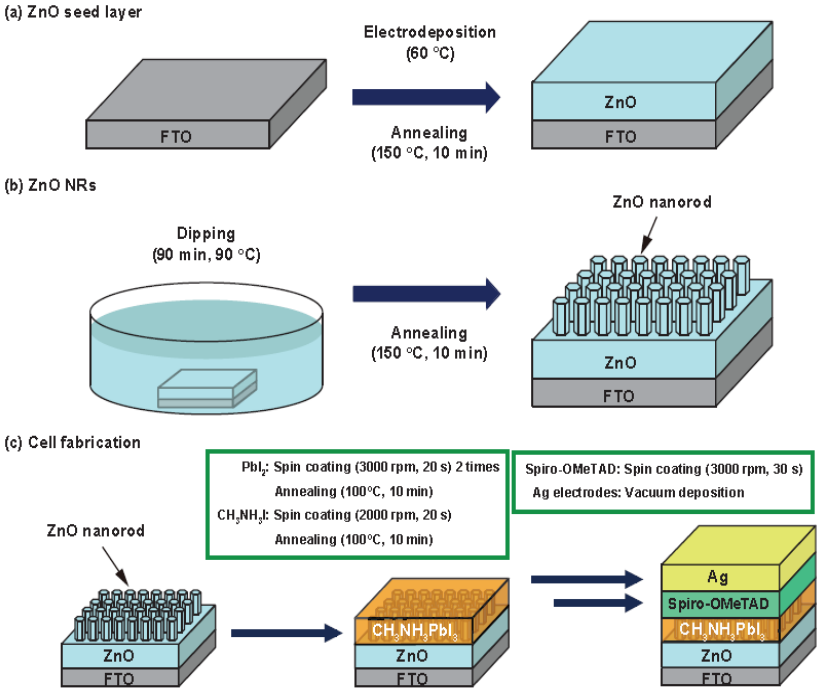


**Figure 8**. Schematic illustrations of fabrication processes of (a) ZnO seed layer, (b) ZnO nanorods, (c) ZnO nanorods/CH3NH3PbI3 SC [60]

The fabrication of the ZnO nanorods perovskite SCs with different lengths of ZnO nanorods were reported by Shirahata et al. [60]. The ZnO nanorods were prepared by chemical bath deposition and directly confirmed to be hexagon shaped nanorods [60]. The lengths of the ZnO nanorods were controlled by deposition condition of ZnO seed layer [60]. The photovoltaic properties of the ZnO nanorods/$CH3NH_3PbI_3$ SCs were investigated by measuring current density voltage characteristics and incident photon to current conversion efficiency [60]. The highest conversion efficiency was obtained in ZnO nanorods/$CH_3NH_3PbI_3$ with the longest ZnO nanorods [60]. The study's results showed that the lengths of the ZnO nanorods could be controlled by deposition time of ZnO seed layer [60]. The conversion efficiencies were improved due to reduction of perovskite structures made from starting materials, and the highest conversion efficiency was obtained in the longest ZnO nanorods/$CH_3NH_3PbI_3$ solar cell [60]. Figure 8 shows the fabrication process of the ZnO nanorods. Figure 9 shows the AFM for the ZnO nanorods [60].

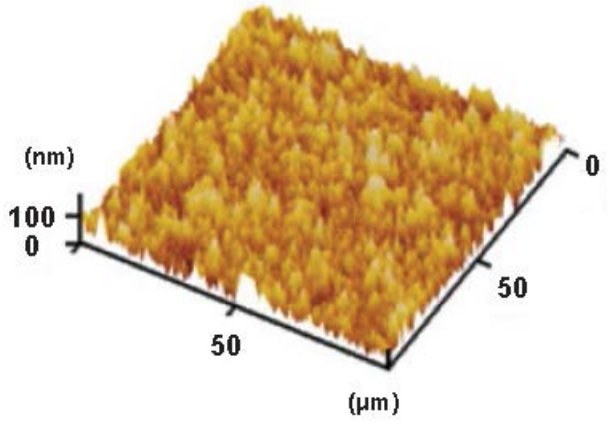


**Figure 9.** AFM images of ZnO seed layers [60]

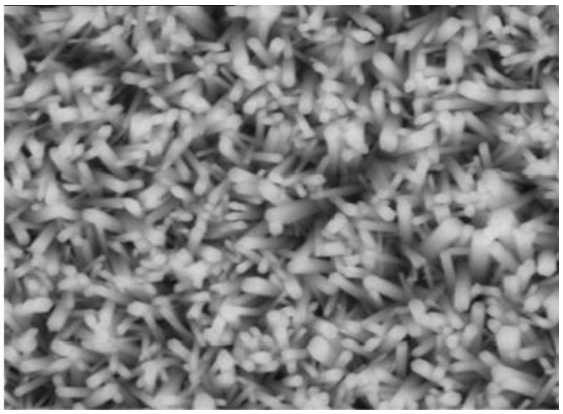

**Figure 10**. SEM images of as-grown ZnO nanorods layers [61]

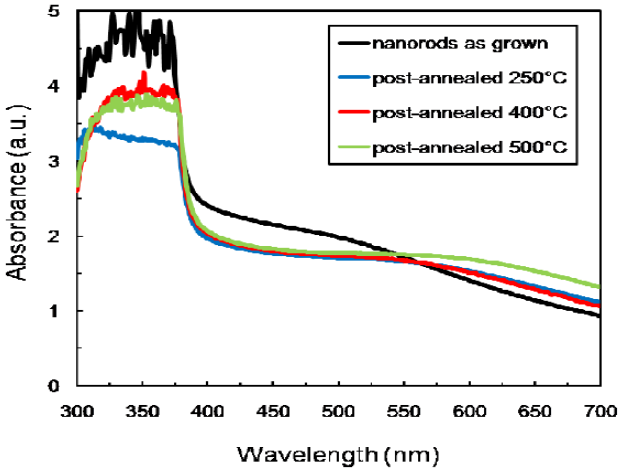


**Figure 11**. UV-vis absorbance spectra of ZnO nanorods [61]

The optical absorbance of the ZnO nanorods was investigated and reported by Mohar et al. [61]. The ZnO thin film were deposited on indium tin oxide layers using

ultrasonic spray pyrolysis method and then grown by hydrothermal method [61]. In order to improve the optical absorbance, the ZnO nanorods were then post-annealed for one hour at three different of temperatures, namely 250, 400, and 500°C [61]. The XRD spectra and FESEM images showed that the ZnO nanorods have the hexagonal wurtzite crystal structure and the increasing of post annealing temperature resulted in the increasing of crystallite size from 38.2 nm to 48.4 nm [61]. The UV-vis spectra showed that all samples of ZnO nanorods exhibited the identical sharp absorption edge at 390 nm indicating that all samples have the same bandgap [61]. The post-annealing process seemed to decreased the optical absorbance in the region of 300-550 nm and increase the optical absorbance in the region of 550-700 nm [61]. The study's results showed that the optical absorbance measurement of ZnO nanorods exhibited the identical sharp absorption edge at 390 nm that indicates that all samples have the same bandgap. The post annealing process at three different temperatures seemed to reduce the native defects in ZnO crystal lattices that can be observed from the decreasing of the optical absorbance in the region of 300-550 nm [61]. Figure 10 shows the SEM for the ZnO nanorods [61]. Figure 11 shows the UV-vis absorbance spectra of ZnO nanorods [61].

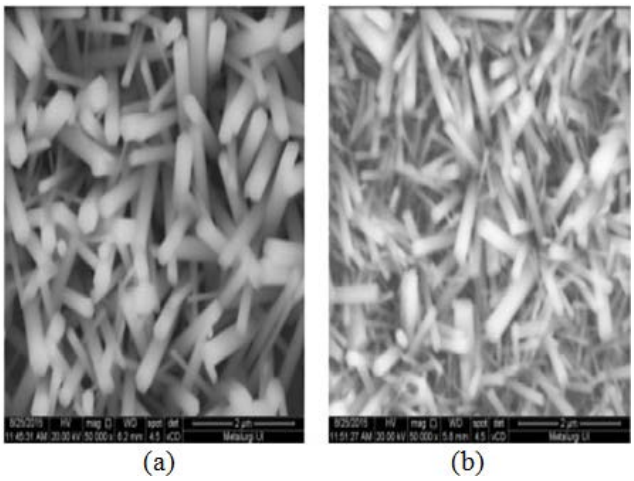


**Figure 12**. FESEM images of ZnO nanorods prepared using growth precursor with a concentration of (a) 0.02 M (b) 0.06 M [62]

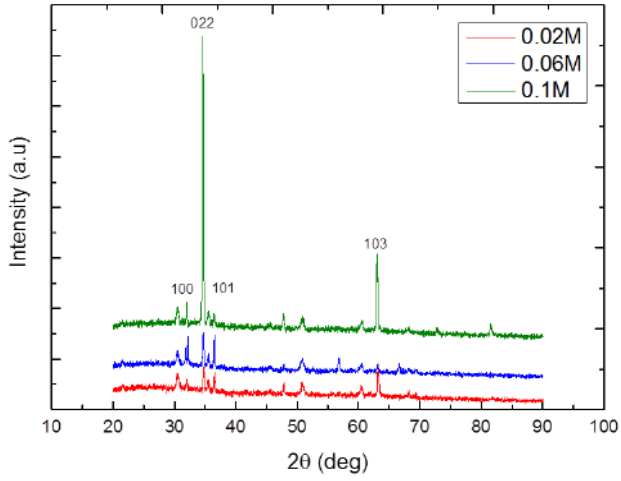


**Figure 13**. XRD pattern of ZnO nanorods prepared using growth precursor with a concentration of 0.02 M, 0.06 M and 0.1 M [62]

The effect of the precursor concentration used in hydrothermal process on the structure, morphology and optical properties ZnO nanorods was investigated and reported by Lestari et al. [62]. The ZnO hexagonal nanorods were synthesized on the indium tin oxide coated glass substrates via hydrothermal process where seed layers were deposited by ultrasonic spray pyrolysis method [62]. The structural and the optical properties of the ZnO nanorods were observed to be influenced by the precursor concentration [62]. The ZnO nanorods were prepared with the highest precursor concentration (0.1 M) showed the structural and optical properties that were rather different from the other samples prepared with 0.02 M and 0.06 M precursor concentrations [62]. The ZnO nanorods were prepared using the 0.1 M precursor were found to grow with larger diameter and more uniformly oriented perpendicularly to the substrate [62]. The diffuse reflectance and PL spectra showed that the increase of precursor concentration results in the decrease of band gap and the increase of emission intensity in UV and orange yellow regions [62]. Figure 12 shows the FESEM images of the ZnO nanorods prepared using growth precursor with a concentration of (a) 0.02 M (b) 0.06 M. Figure 13 shows the XRD pattern of ZnO nanorods prepared using growth precursor with a concentration of 0.02 M, 0.06 M and 0.1 M [62].

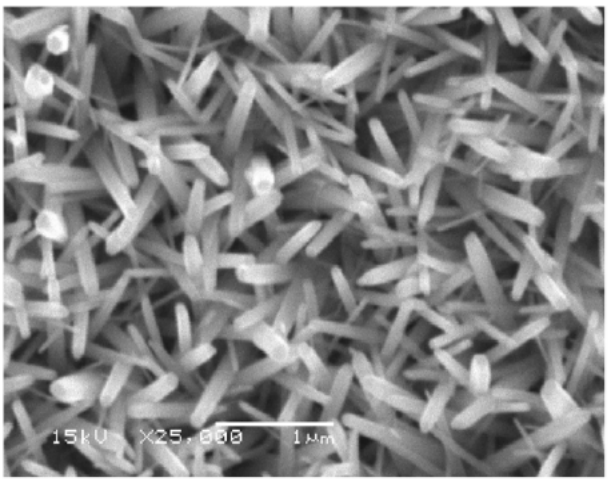


**Figure 14.** SEM of ZnO nanorods [63]

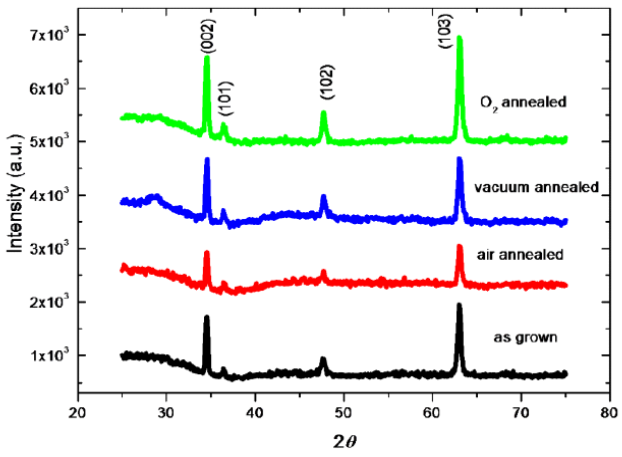


**Figure 15**. XRD spectra of as-grown ZnO nanorods and annealed in various gas ambient [63]

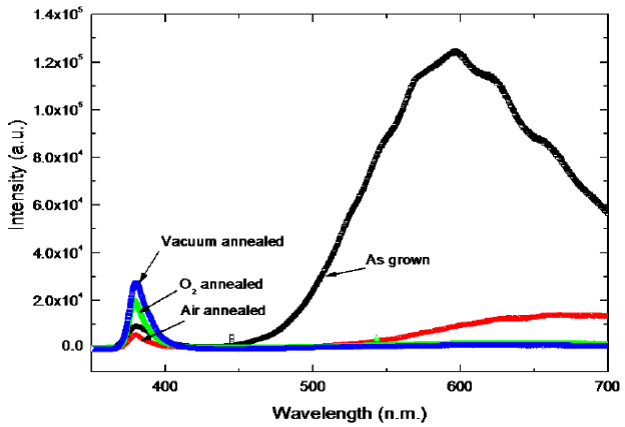


**Figure 16**. Room temperature PL of as-grown ZnO nanorods and annealed in various conditions [63]

The PL properties of the ZnO nanorods fabricated by a hydrothermal reaction on silicon substrate were investigated and reported by Iwan et al. [63]. The ZnO seed layer was fabricated by depositing ZnO thin films on Si substrates by ultrasonic spray pyrolisis (USP) [63]. The annealing effects on the crystal structure and optical properties of ZnO nanorods were investigated [63]. The post annealing treatment was performed at 800°C with different environments [63]. The resulted ZnO nanorods were characterized by XRD and PL in order to analyze crystal structure and optical properties, respectively [63]. The results of that study showed the orientations of [002], [101], [102], and [103] diffraction peaks were observed and hexagonal wurtzite structure of ZnO nanorods were vertically grown on Si substrates [63]. The room temperature PL spectra show UV and visible emissions [63]. The annealed ZnO nanorods in vacuum condition ($3.8 \times 10^{-3}$ Torr) has dominant UV emission [63]. Meanwhile, non-annealed of ZnO nanorods have dominant visible emission [63]. It was expected that the annealed of ZnO in vacuum condition suppresses the existence of native defects in ZnO nanorods [63]. The annealed ZnO in vacuum condition suppressed the existence of native defects in ZnO nanorods [63]. The study's result also showed that the vertically ZnO nanorods grown on Si substrates had a hexagonal wurtzite structure [63]. The room temperature PL spectra of ZnO nanorods showed UV and visible emissions [63]. Figure 14 shows the SEM of the ZnO nanorods [63]. Figure 15 shows the XRD of the ZnO nanorods [63]. Figure 16 shows the room temperature PL of as-grown and annealed ZnO nanorods in various conditions [63].

The Al doping's influence on the morphological and the optical properties of the ZnO nanorod was investigated and reported by Mohamed et al. [64]. The ZnO was grown on glass substrate [64]. The ZnO with different Al doping percentage was synthesis by sol gel immersion method [64]. The ZnO was doped with Al doped at various doping percentage from 1 to 5 [64]. It was found that with different Al percentage influence the morphological and optical properties of ZnO growth [64]. The FESEM image showed that the use of different Al doping causes the difference in geometry and size of ZnO nanorods growth [64]. Based on the UV-Vis spectroscopy, the transmittance at 1% Al doping has the highest spectrum [64]. Based on the UV-Vis analysis, the transmittance of the ZnO thin films shifted towards higher wavelength [64]. The transmittance decreased with the increasing of the Al doping percentage [64]. It was found that the diameter size of the ZnO thin films increased as the percentage of Al doping increased [64]. The optical properties showed a good transmittance of the ZnO thin films at low Al doping percentage [64]. The evolution of the geometry, diameter size and good optical properties of thin films may be good to use in the sensor application [64]. Figure 17 shows the SEM of the ZnO nanorods [64]. Figure 18 shows the average diameter size of the ZnO nanorods for 1% to 5% doping [64]. Figure 19 shows the transmittance spectra of the ZnO nanorods for 1% to 5% doping [64].

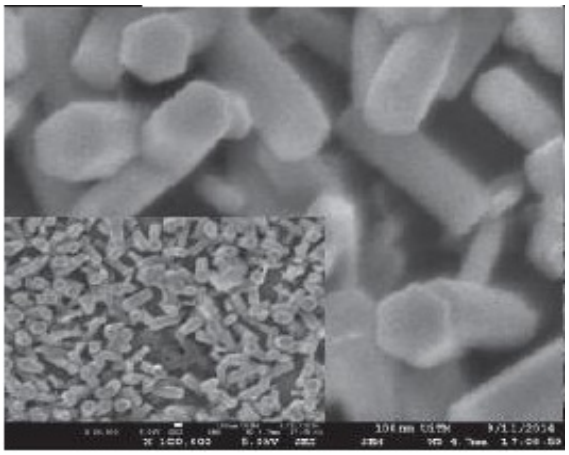

**Figure 17**. SEM of ZnO nanorods [64]

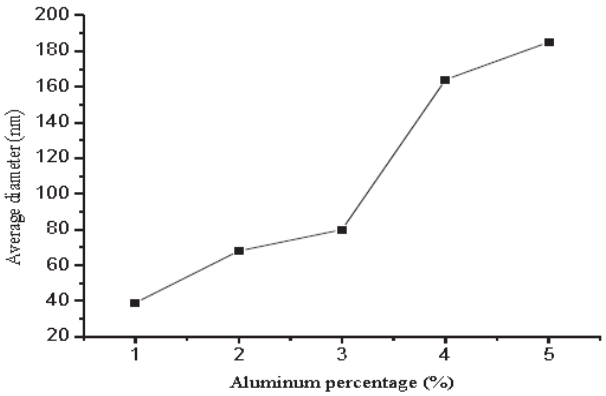


**Figure 18**. Average diameter size of ZnO nanorods for 1% to 5% doping [64]

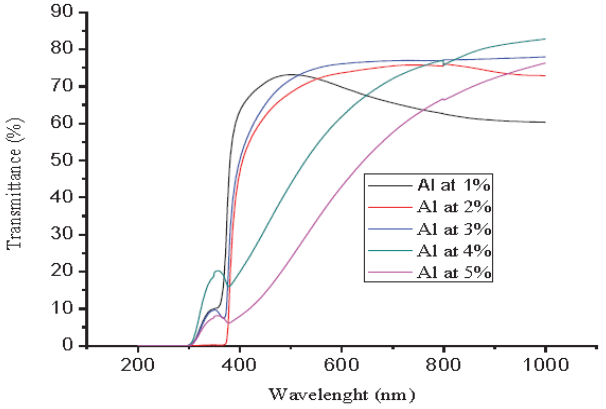


**Figure 19**. Transmittance spectra of ZnO nanorods for 1% to 5% doping [64]

# 5. Conclusion

In conclusion, recent advances of the ZnO based nanowires and nanorods were presented and discussed. ZnO has been extensively studied over the past decade. Many great efforts have been intensified for understanding the optical and the electrical properties. ZnO based nanostructured including nanowires and nanorods have a promising potential in many areas. Despite the progress of the ZnO of nanowires and nanorods, a lack of p-type doping is still a challenging task. On the other hand, the p-type doping levels in epitaxial films still require even better control of the background n-type conductivity in the material that arises from native defects and impurities such as hydrogen. Also, the development of the implant doping processes, to realize both n-type and p-type layers is still requiring a better understanding of the defects created by the implant step and their thermal stability and also a better understanding of the stability of the ZnO surface during activation annealing. Moreover, high quality ZnO nanowires with a well-controlled structures and properties are still difficult to be performed. Finally, ZnO and GaN are promising future compounds semiconductor materials over other materials.

# References


[1] Khan, I., Khan, S., Nongjai, R., Ahmed, H., and Khan, W., "Hydrothermal synthesis of zinc oxide powders with controllable morphology," *Optical Materials*, 35. 1189-1193. 2013.

[2] Xu, H., Wang, H., Zhang, Y., He, W., Zhu, M., Wang, B., and Yan, H., "Structural and optical properties of gel-combustion synthesized Zr doped ZnO nanoparticles," *Ceramics International*, 30. 93-97. 2004.

[3] Kung, S., and Sreenivas, K., "Defect free C-axis oriented zinc oxide (ZnO) films grown at room temperature using RF magnetron sputtering," *AIP Conference Proceedings*, 1731. 1-3. 2016.

[4] Li, Y., Bando, Y., and Golberg, D., "ZnO nanoneedles with tip surface perturbations: Excellent field emitters," Applied Physics Letters, 84. 3603. 2004.

[5] Saito, M., and Fujihara, S., "Large photocurrent generation in dye-sensitized ZnO solar cells," *Energy & Environmental Science*, 1. 280-283. 2008.

[6] Zhou, J., Wu, X., Xiao, D., Zhuo, M., Jin, H., Luo, J., and Fu, Y., "Deposition of aluminum doped ZnO as electrode for transparent ZnO/glass surface acoustic wave devices," *Surface and Coatings Technology*, 320. 39-46. 2017.

[7] Choi, Y., Kang, J., Hwang, D., and Park, S., "Recent advances in ZnO based light-emitting diodes," *IEEE Transactions on Electronic Devices*, 57. 26-41. 2010.

[8] Zhang, M., Gao, X., Barra, A., Chang, P., Huang, L., Hellwarth, R., and Lu, J., "Core-shell structured Si/ZnO photovoltaics," *Materials Letters*, 140. 59-63. 2015.

[9] Hossaini, H., Moussavi, G., and Farrokhi, M., "Oxidation of diazinon in cns-ZnO/LED photocatalytic process: Catalyst preparation, photocatalytic examination, and toxicity bioassay of oxidation by products," *Separation and purification technology*, 174. 320-330. 2017.

[10] Sabah, M., Hassan, Z., Naser, M., Al-hardan, H., and Bououdina, M., "Fabrication of low cost UV photo detector using ZnO nanorods grown onto nylon substrate," *Journal of Materials Science*, 26. 1322-1331. 2015.

[11] Pandya, H., Chandra, S., and Vyas, A., "Integration of ZnO nanostructures with MEMS for ethanol sensor," *Sensors and Actuators B, Chemical*, 161. 923-928. 2012.

[12] Taube, A., Sochacki, M., Kwietniewski, N., Werbowy, A., Gierałtowska, S., Wachnicki, L., Godlewski, M., and Szmidt, J., "Electrical properties of isotype and anisotype ZnO/4H-SiC heterojunction diodes," *Applied Physics Letters*, 110. 1120-1124. 2017.

[13] Sin, L., Arshad, M., Fathil, M., Adzhri, R., Nuzaihan, N., Ruslinda, A., Gopinath, S., and Hashim, U., "Zinc oxide interdigitated electrode for biosensor application," *AIP Conference Proceedings*, 1733. 020075. 2016.

[14] Tvarozek, V., Shtereva, K., Novotny, I., Kovac, J., Sutta, P., Srnanek, R., and Vincze, A., "RF diode reactive sputtering of n- and p-type zinc oxide thin films," *Vacuum*, 82. 166-169. 2007.

[15] Liu, G., Rahman, E., and Ban, D., "Performance optimization of p-n homojunction nanowire based piezoelectric nanogenerators through control of doping concentration," *Journal of Applied Physics*, 118. 094307. 2017.

[16] Humid, H., and Celik-Butler, Z., "Li-ZnO nanowire carpet as a micro-newton force sensor with nanometer res," *IEEE Sensors Conferences*, 1-3. 2017.

[17] Pemmaraju, C., Archer, T., Hanafin, R., and Sanvito, S., "Investigation of n-type donor defects in Co-doped ZnO," *Journal of Magnetism and Magnetic Materials*, 316. e185-e187. 2007.

[18] Saroj, R., and Dhar, S., "Relationship between dislocation and the visible luminescence band observed in ZnO epitaxial layers grown on c-plane p-GaN templates by chemical vapor deposition technique," *Journal of Applied Physics*, 120. 075701. 2016.

[19] Urgessa, N., Dobson, S., Talla, K., Murape, D., Venter, A., and Botha, J., "Optical and electrical characteristics of ZnO/Si heterojunction," *Physica B, Condensed Matter*, 439. 149-152. 2014.

[20] Alivov, R., Kalinina, E., Cherenkov, A., Look, D., Ataev, B., Omaev, A., Chukichev, M., and Bagnall, D., "Fabrication and characterization of n-ZnO/p-AlGaN n-ZnO/p-AlGaN heterojunction light-emitting diodes on 6H-SiC substrates," *Applied Physics Letters*, 83. 4719. 2003.

[21] Alvi, N., Riaz, M., Tzamalis, G., Nur, O., and Willander, M., "Fabrication and characterization of high-brightness light emitting diodes based on n-ZnO nanorods grown by a low-temperature chemical method on p-4H-SiC and p-GaN," *Semiconductor Science and Technology*, 25. 065004. 2010.

[22] Li, Y., and Meng, J., "Al-doping effects on structure and optical properties of ZnO nanostructures," *Journal of Materials letters*, 117. 260-262. 2014.

[23] Chaabouni, Y., Khalfallah, B., and Abaab, M., "Doping Ga effect on ZnO radio frequency sputtered films from a powder target," *Thin Solid Films*, 617. 95-102. 2016.

[24] Ahmad, M., Zhao, J., Iqbal, J., Miao, W., Xie, L., Mo, R., and Zhu, J., "Conductivity enhancement by slight indium doping in ZnO nanowires for optoelectronic applications," *Journal of Physics D: Applied Physics*, . 0022-3727. 2009.

[25] Chen, Y., Huang, I., Chang, S., and Hsueh, T., "Photodetector of ZnO nanowires based on through-silicon via approach," *IEEE International Interconnect Technology Conference/Advanced Metallization Conference (IITC/AMC)*, 123-124. 2016.

[26] Yi, G., Wang, C., and Park, W., "ZnO nanorods: synthesis, characterization and applications," *Semiconductor Science and Technology*, 20. S22-S34. 2005.

[27] Tan, S., Umar, A., Balouch, A., Yahaya, M., Yap, C., Salleh, M., and Oyama, M., "ZnO nanocubes with (101) basal plane photocatalyst prepared via a low-frequency ultrasonic assisted hydrolysis process," *Ultrasonics Sonochemistry*, 21. 754-760. 2014.

[28] Pan, Z., Dai, Z., and Wang, Z., "Nanobelts of semiconducting oxides," *Science*, 291. 1947-1949. 2001.

[29] Jianming, J., Xiaoqin, F., and Guibin, C., "Electromechanical properties of a zigzag ZnO nanotube under local torsion," *Journal of Nanoparticle Research*, 15. 1-9. 2013.

[30] Bhavsar, K., Ross, D, Prabhu, R., and Pollard, P., "LED-controlled tuning of ZnO nanowires' wettability for biosensing applications," Nano Reviews, 6. 1-6. 2015.

[31] Logothetidis, S., Laskarakis, A., Kassavetis, S., Lousinian, S., Gravalidis, C., and Kiriakidis, G., "Optical and structural properties of ZnO for transparent electronics," *Thin Solid Films*, 516. 1345-1349. 2008.

[32] Pal, A., and Mohan, D., "Multi-angle ZnO microstructures grown on Ag nanorods array for plasmon-enhanced near-UV-blue light emitter," *Nanotechnology*, 28. 415707-415707. 2017.

[33] Serhane, R., Messaci, S., Lafane, S., Khales, H., Aouimeur, W., Bey, A., and Boutkedjirt, T., "Pulsed laser deposition of

piezoelectric ZnO thin films for bulk acoustic wave devices," *Applied Surface Science*, 288. 572-578. 2014.

[34] Nie, Y., Deng, P., Zhao, Y., Wang, P., Xing, L., Zhang, Y., and Xue, X., "The conversion of PN-junction influencing the piezoelectric output of a CuO/ZnO nanoarray nanogenerator and its application as a room-temperature self-powered active $H_2S$ sensor," *Nanotechnology*, 25. 265501. 2014.

[35] Tan, Q., Wang, J., Zhong, X., Zhou, Y., Wang, Q., Zhang, Y., Zhang, X., and Huang, S., "Impact of ZnO Polarization on the characteristics of metal-ferroelectric-ZnO field effect transistor," *IEEE Transactions on Electron Devices*, 58. 2738-2742. 2011.

[36] Fail, P., and Furtado, C., "Effect of composition on electrical response to humidity of TiO2:ZnO sensors investigated by impedance spectroscopy," *Sensors and Actuators B: Chemical*, 181. 720-729. 2013.

[37] Panda, D., and Tseng, T., "One-dimensional ZnO nanostructures: fabrication, optoelectronic properties, and device applications," *Journal of Materials Science*, 48. 6849-6877. 2013.

[38] Zhao, Q., Huang, C., Zhu, R., Xu, J., Chen, L., and Yu, D., "2D planar field emission devices based on individual ZnO nanowires," *Solid State Communications*, 151. 1650-1653. 2011.

[39] Lokman, A., Arof, H., Wadi, S., Harith, Z., Rafaie, H., and Nor, R., "Optical fiber relative humidity sensor based on Inline Mach-Zehnder interferometer with ZnO nanowires coating," *IEEE Sensors Journal*, 16. *312*-316. 2016.

[40] Willander, M., and Klason, P., "ZnO nanowires: Chemical growth, electrodeposition, and application to intracellular nano-sensors," *Physica Status Solidi*, C 5. 3076-3083. 2008.

[41] Lupan, O., Emelchenko, G., Ursaki, V., Chai, G., Redkin, A., Gruzintsev, A., Tiginyanu, I., Chow, L., Ono, L., Cuenya, B., Heinrich, H., and Yakimov, E., "Synthesis and characterization of ZnO nanowires for nanosensor applications," *Materials Research Bulletin*, 45.1026-1032. 2010.

[42] Ramgir, N., Kaur, M., Sharma, P., Datta, N., Kailasaganapathi, S., Bhattacharya, S., Debnath, A., Aswal, D., and Gupta, S., "Ethanol sensing properties of pure and Au modified ZnO nanowires," *Sensors and Actuators. B, Chemical*, 187. 313-318. 2013.

[43] Zhao, Q., Klason, P., and Willander, M., "Growth of ZnO nanostructures by vapor liquid solid method," *Applied Physics A*, 88. 27-30. 2007.

[44] Pan, M., Fenwick, W., Strassburg, M., Li, N., Kang, H., Kane, M., Asghar, A. Gupta, S., Varatharajan, R., Nause, J., El-Zein, N., Fabiano, P., Steiner, T., and Ferguson, I., "Metal organic chemical vapor deposition of ZnO," *Journal of Crystal Growth*, 287. 688-693. 2006.

[45] Chiu, S., and Huang, J., "Chemical bath deposition of ZnO and Ni doped ZnO nanorod," *Journal of Non-Crystalline Solids*, 358. 2453-2457. 2012.

[46] Polsongkram, D., Chamninok, P., Pukird, S., Chow, L., Lupan, O., Chai, G., Khallaf, H., Park, S., and Schulte, A., "Effect of synthesis conditions on the growth of ZnO nanorods via hydrothermal method," *Physica B: Condensed Matter*, 403. 3713-3717. 2008.

[47] Wang, L., Chauveau, J., Brenier, R., Sallet, V., Jomard, F., Sartel, C., and Bremond, G., "Access to residual carrier concentration in ZnO nanowires by calibrated scanning spreading resistance microscopy," *Applied Physics Letters*, 108. 108-112. 2016.

[48] Yadav, L., Mehta, B., and Singh, J., "Effect of gaseous atmosphere on photoinduced water wetting of ZnO nanowires," *AIP Conference Proceedings*, 1731. 080044. 2016.

[49] Jabri, S., Souissi, H., Lusson, A., Sallet, V., Meftah, A., Galtier, P., and Oueslati, M., "The ratio Oxygen/Zinc effect on photoluminescence emission line at 3.31 eV in ZnO nanowires," *Journal of Applied Physics*, 119. 205710. 2016.

[50] Akgul, G., and Akgul, F., "Fabrication and characterization of Ga-doped ZnO/Si heterojunction nanodiodes," *AIP Conference Proceedings*, 1815. 110001. 2017.

[51] Shoaee, S., Briscoe, J., Durrant, J., and Dunn, S., "Acoustic enhancement of polymer/ZnO nanorod photovoltaic device performance," *Advanced Materials*, 26. 263-268. 2014.

[52] Long, H., Fang, G., Li, S., Mo, X., Wang, H., Huang, H., Jiang, Q., Wang, J., and Zhao, X., "A ZnO/ZnMgO multiple quantum well ultraviolet random laser diode," *IEEE Electron Device Letters*, 32. 54-56. 2011.

[53] Hwang, J., Wang, F., Kung, C., and Chan, M., "Using the surface plasmon resonance of Au nanoparticles to enhance ultraviolet response of ZnO nanorods based schottky barrier photodetectors," *IEEE Transactions on Nanotechnology*, 14. 318-321. 2015.

[54] Sipr, O., and Rocca, F., "Zn K edge and O K edge x-ray absorption spectra of ZnO surfaces: Implications for nanorods," *Journal of Physics: Condensed Matter*, 23. 315501. 2011.

[55] Yang, J., Wang, Y., Kong, J., Yu, M., and Jin, H., "Synthesis of Mg-doped hierarchical ZnO nanostructures via hydrothermal method and their optical properties," Journal of alloys and compounds, 657. 261-267. 2016.

[56] Montenegro, D., Souissi, A., Tomas, C., Sanjose, V., and Sallet, V., "Morphology transitions in ZnO nanorods grown by MOCVD," *Journal of Crystal Growth*, 359. 122-128. 2012.

[57] Mendelsberg, R., Kerler, M., Durbin, S., and Reeves, R., "Photoluminescence behavior of ZnO nanorods produced by eclipse PLD from a Zn metal target," *Superlattices and Microstructures*. 43. 594-599. 2008.

[58] Sang, N., Beng, T., Jie, T., Fitzgerald, E., and Jin, C., "Fabrication of p-type ZnO nanorods/n-GaN film heterojunction ultraviolet light emitting diodes by aqueous solution method," *Physica Status Solidi*. A 210. 1618-1623. 2013.

[59] Mustafa, M., Iqbal, Y., Majeed, U., and Sahdan, M., "Effect of precursor's concentration on structure and morphology of ZnO nanorods synthesized through hydrothermal method on gold surface," *AIP Conference Proceedings*, 1788. 030120. 2017.

[60] Shirahata, Y., Tanaike, K., Akiyama, T., Fujimoto, K., Suzuki, A., Balachandran, J., and Oku, T., "Fabrication and photovoltaic properties of ZnO nanorods/perovskite solar cells," *AIP Conference Proceedings*, 1709. 020018. 2016.

[61] Mohar, R., Iwan,S., Djuhana, D., Imawan, C., Harmoko, A., and Fauzia, V., "Post-annealing effect on optical absorbance of hydrothermally grown zinc oxide nanorods," *AIP Conference Proceedings*, 1729. 020024. 2016.

[62] Lestari, A., Iwan, S., Djuhana, D., Imawan, C., Harmoko, A., and Fauzia, V., "Effect of precursor concentration on the structural and optical properties of ZnO nanorods prepared by hydrothermal method," *AIP Conference Proceedings*, 1729. 020027. 2016.

[63] Iwan, S., Fauzia, V., Umar, A., and Sun, X., "Room temperature photoluminescence properties of ZnO nanorods grown by hydrothermal reaction," *AIP Conference Proceedings*, 1729. 020031. 2016.

[64] Mohamed, R., Ismail, A., Khusaimi, Z., Mamat, M., Alrokayan, S., Khan, H., and Rusop, M., "Percentage of different aluminum doping influence the morphological and optical properties of ZnO nanostructured growth for sensor application," *AIP Conference Proceedings*, 1733. 020061. 2016.